Thermochimica Acta, 12 (1975) 323–335

RELATIONS BETWEEN THERMODYNAMIC, PHYSICAL AND STRUCTURAL PROPERTIES OF ALKALI HALIDES AT THEIR MELTING POINTS

J. LIELMEZS

Chemical Engineering Department, The University of British Columbia, Vancouver, B.C. (Canada)

(Received 6 March 1975)

ABSTRACT

Linear relations of the general form $A = a + m\tau$ have been presented to describe the connection between the characteristic energetic and geometric parameters of alkali halides at their respective melting points. Inference has been made that these presented relations may be associated with the structure of the alkali halide liquids.

INTRODUCTION

Melting, the change of substance from the solid into the liquid state, is a very complex phenomenon, and so there exist many microscopic and phenomenological attempts to derive theoretically[1–8] a description of this state change, or the laws of melting. Despite the existence of these many, apparently uncorrelated approaches to this problem, there still could be noted a common feature if we relate the heat of melting to a set of measurable thermodynamic, physical and structural properties of substance. Then, in effect we have described the energetics associated with the melting process through the same species molecular force interaction patterns found within the substance. For instance, in its simplest form such a relation is the Clausius–Clapeyron differential equation governing the coexistence curve of two-phase equilibria. In this work, however, no attempt has been made to present theoretical derivations stemming from the fundamental principles. Rather, at this point, the experimental data of alkali halides have been reassessed empirically to determine what properties would directly affect the melting process of these simple ionic substances.

CORRELATION

If we introduce two dimensionless coordinates, A and τ, where A represents any of the following ratios (compare with Table 1):

$$\ln\left(\frac{\Delta H_f(\alpha_c/\alpha_a)}{RT_f}\right); \quad \ln\left(\frac{U_0(\alpha_c/\alpha_a)}{RT_f}\right); \quad \ln\left(\frac{\Delta H_f(\alpha_c/\alpha_a)}{R\Delta T}\right);$$

$$\ln\left(\frac{U_0(\alpha_c/\alpha_a)}{R\Delta T}\right); \quad \ln\left(\frac{hc\omega_e}{kT_f}\right); \quad \ln\left(\frac{hc\omega_e}{k\Delta T}\right); \tag{1}$$

and τ on the other hand is any one of the following entities:

$$\ln\left(\frac{V_m^s}{V_m^l}\right); \qquad \ln\left(\frac{r_c}{r_a}\right); \qquad \ln\left(\frac{hc\omega_e}{kT_f}\right); \qquad \ln\left(\frac{hc\omega_e}{k\Delta T}\right) \tag{2}$$

then it is possible to establish linear relations between Λ and τ for selected groups of these coordinates (eqns (1), (2); Figs. 1–4, Table 1), i.e.:

$$\Lambda = a + m\tau \tag{3}$$

such that a and m are characteristic constants (slope and intercept, respectively) for each of the listed coordinate set groupings of the given alkali halides.

To establish this correlation set (eqn (3)); the any two chosen Λ–τ dimensionless parameter groups were calculated for each alkali halide class (Table 1) using the thermodynamic, physical and structural alkali halide property values as found in Table 2.

To establish the separate alkali halide class equations of the form of eqn (3), the values of a and m for 14 Λ–τ coordinate sets representing all given alkali halide classes (MX, such that M = Li, Na, K, Rb, SCs and X = F, Cl, Br, I) were obtained

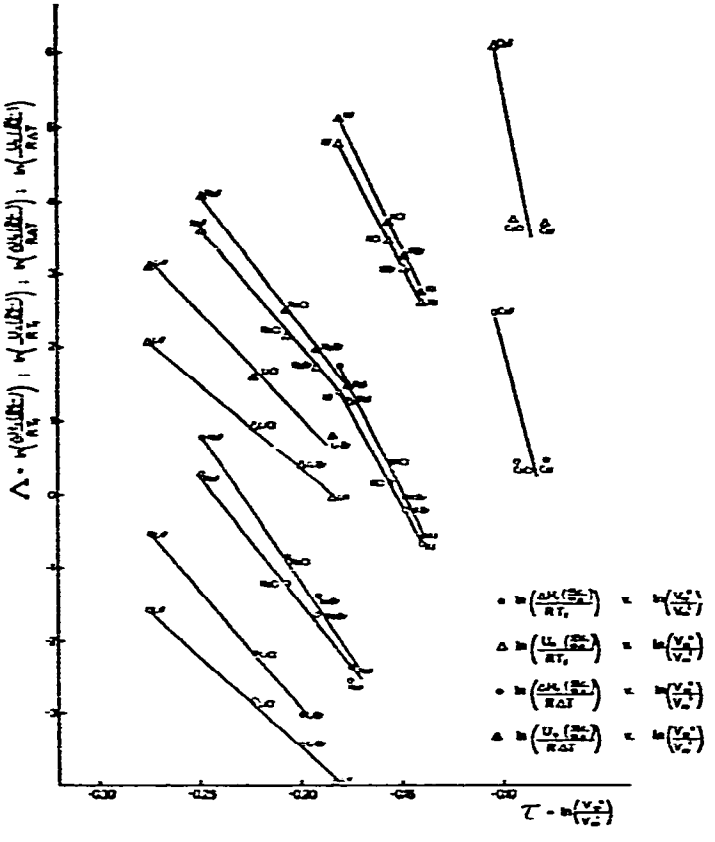

Fig. 1. Plot of Λ–τ coordinates for groups I–IV (Table 1).

by means of linear least square curve fitting techniques. The calculated a and m values are found in Table 3. The high correlation coefficient r values computed for each of the alkali halide line equations (Table 3) indicate a relatively high degree of goodness of curve fit for the proposed correlation.

DISCUSSION

Considering the chosen Λ–τ coordinates (Table 1), we note that for the alkali halide series, MX (M = Li, Na, K, Rb, Cs and X = F, Cl, Br, I), the natural logarithm of the dimensionless ratios (eqn 1) when plotted against the natural logarithm of the geometrical ratios (eqn 2) yields straight line relations (Figs. 1–4, Table 3). This, however, occurs only when the heat of melting, ΔH_f and the crystal lattice energy U_0, is multiplied by the effective electronic polarizability ratio*, α_c/α_a, of the given alkali halide.

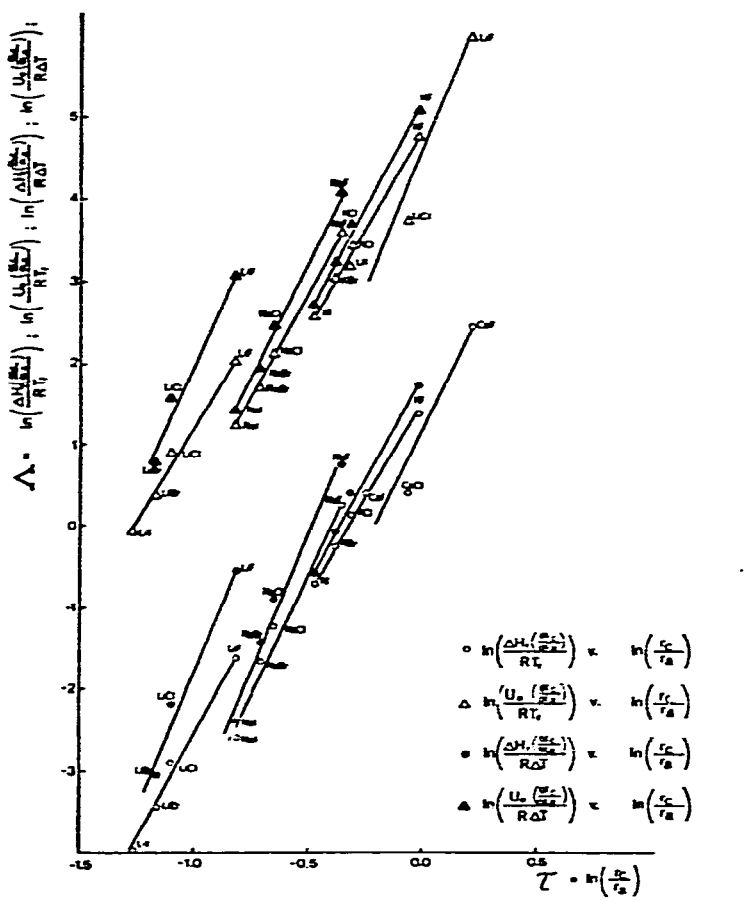

Fig. 2. Plot of Λ–τ coordinates for groups V–VIII (Table 1).

*The effective electronic polarizability values taken from the collection of data by Brumer and Karplus[9].

On the other hand, the radiation energy, $hc\omega_c$, divided by the thermal energy at the melting point, kT_f; or, again when divided by the difference in thermal energy between the melting temperature, T_f, and the Debye temperature, θ, forming $k\Delta T$; directly correlates with the natural logarithm of ionic radius, r_c/r_a, or again the volume, V_m^s/V_m^l, ratios*.

Pauling[10] has argued that the irregular pattern found in the alkali halide melting point sequences (Table 2) are attributable to the ionic radius-ratio effect. Fajans[14] alternately has stressed that these alkali halide melting point irregularities are due to deformation of ions.

Yet, both the observed alkali halide melting point anomalies (Table 2) and our proposed energetic–geometrical property relations (eqns (1)–(3); Figs. 1–4, Table 3) reflect the common various interionic force field changes occurring during the melting process of alkali halides. Recalling that the proposed Λ–τ correlations contain the effective polarizability (modifying property) ratio, α_c/α_a; and the ionic radius (cor-

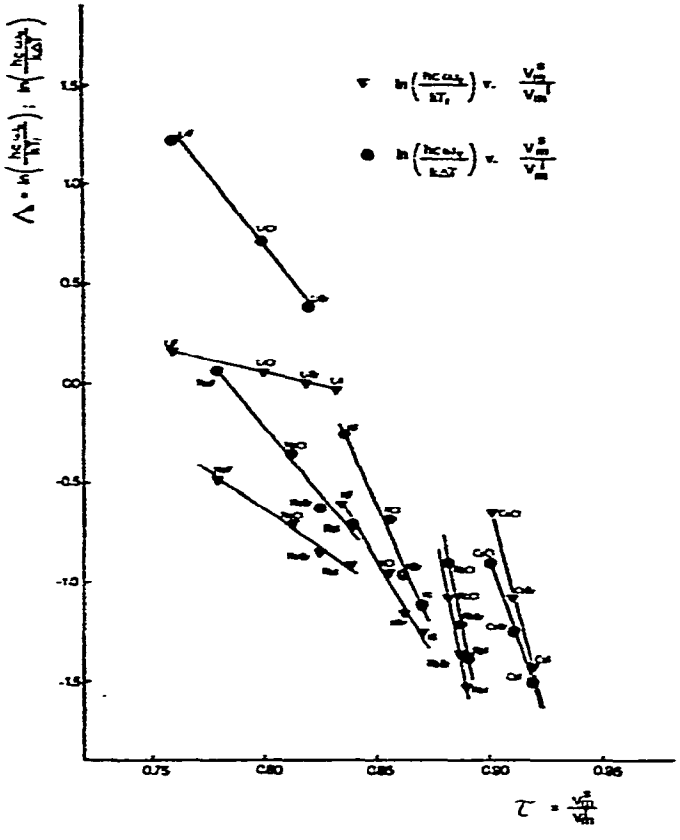

Fig. 3. Plot of Λ–τ coordinates for groups IX and X (Table 1).

*Earlier use of the dimensionless coordinate $\Lambda = \ln hc\omega_e/kT$ was made by Lielmezs and his co-workers[11–13] in the study of properties describing the vaporization process.

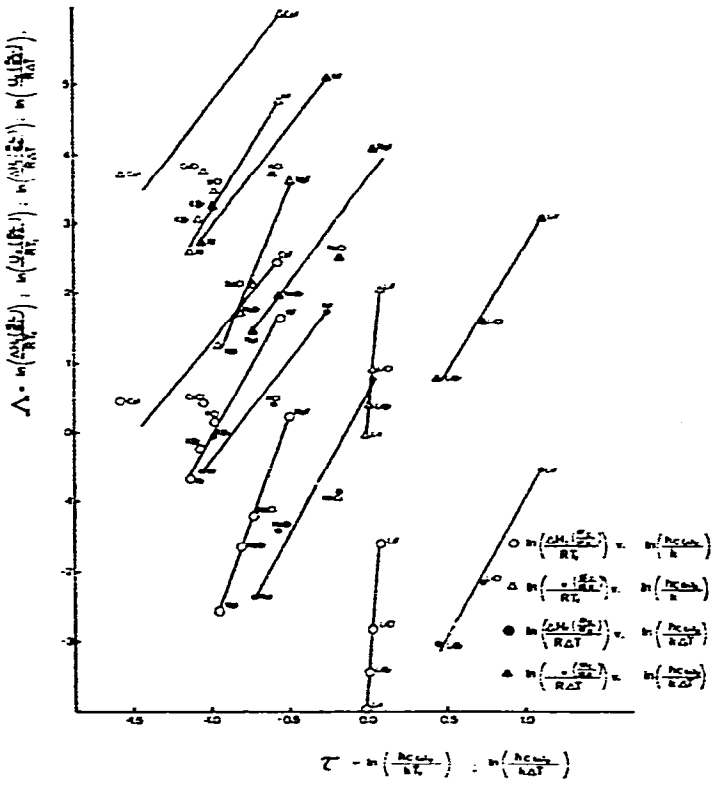

Fig. 4. Plot of Λ–τ coordinates for groups XI–XIV (Table 1).

relating property) ratio, r_c/r_a; we can state rather assuredly that our obtained Λ–τ relations (eqn (3), Figs. 1–4, Table 3) include both Pauling[10] and Fajans[14] views, suggesting realistically which energetic–geometric properties might determine the behavior of the alkali halide melting process.

If so, then the combination of both, the Pauling's[10] ionic radius ratio concept, and Fajans[14] ion deformation theory as expressed through the effective electron polarizability ratios would describe effectively the interionic equilibrium found during the melting process of alkali halides.

This interdependence between the ionic radius and the electronic polarizability is indicated by comparing the formula for calculating the ionic radius of isoelectronic ions[10]

$$r = \frac{C}{Z-S} \tag{4}$$

with the Born–Heisenberg[15] formula used to calculate individual electronic polarizabilities:

$$\alpha_j = \frac{C'}{Z_i - S_i} \tag{5}$$

TABLE 1

COORDINATE GROUPS (eq (3))

Group	*A*	τ	*Group*	*A*	τ
II	$\ln\left(\frac{\Delta H_f(\alpha_c/\alpha_a)}{RT_f}\right)$	$\ln\left(\frac{V_m^s}{V_m^l}\right)$	VIII	$\ln\left(\frac{U_0(\alpha_c/\alpha_a)}{R\Delta T}\right)$	$\ln\left(\frac{r_c}{r_a}\right)$
III	$\ln\left(\frac{U_0(\alpha_c/\alpha_a)}{RT_f}\right)$	$\ln\left(\frac{V_m^s}{V_m^l}\right)$	IX	$\ln\left(\frac{hc\omega_e}{kT_f}\right)$	$\ln\left(\frac{V_m^s}{V_m^l}\right)$
III	$\ln\left(\frac{\Delta H_f(\alpha_c/\alpha_a)}{R\Delta T}\right)$	$\ln\left(\frac{V_m^s}{V_m^l}\right)$	X	$\ln\left(\frac{hc\omega_e}{k\Delta T}\right)$	$\ln\left(\frac{V_m^s}{V_m^l}\right)$
IV	$\ln\left(\frac{U_0(\alpha_c/\alpha_a)}{R\Delta T}\right)$	$\ln\left(\frac{V_m^s}{V_m^l}\right)$	XI	$\ln\left(\frac{\Delta H_f(\alpha_c/\alpha_a)}{RT_f}\right)$	$\ln\left(\frac{hc\omega_e}{kT_f}\right)$
V	$\ln\left(\frac{\Delta H_f(\alpha_c/\alpha_a)}{RT_f}\right)$	$\ln\left(\frac{r_c}{r_a}\right)$	XII	$\ln\left(\frac{U_0(\alpha_c/\alpha_a)}{RT_f}\right)$	$\ln\left(\frac{hc\omega_e}{kT_f}\right)$
VI	$\ln\left(\frac{U_0(\alpha_c/\alpha_a)}{RT_f}\right)$	$\ln\left(\frac{r_c}{r_a}\right)$	XIII	$\ln\left(\frac{\Delta H_f(\alpha_c/\alpha_a)}{R\Delta T}\right)$	$\ln\left(\frac{hc\omega_e}{k\Delta T}\right)$
VII	$\ln\left(\frac{\Delta H_f(\alpha_c/\alpha_a)}{R\Delta T}\right)$	$\ln\left(\frac{r_c}{r_a}\right)$	XIV	$\ln\left(\frac{U_0(\alpha_c/\alpha_a)}{R\Delta T}\right)$	$\ln\left(\frac{hc\omega_e}{k\Delta T}\right)$

As a matter of fact, by calculation it can be shown that crystal ionic polarizabilities and the cubes of the crystal ionic radii very closely correspond to each other[15].

Because of the existing alkali halide ionic force interactions at the melting point, our correlations, instead of Pauling's[10] free ion electronic polarizability values, incorporate the effective polarizability ratios.

The values of both of these types of polarizabilities differ considerably. For instance, using Brumers and Karplus[9] suggested effective electronic polarizability values, on the average, the polarizability of the positive ion has been increased by a factor of 1.29 and the polarizability of the negative ion has been decreased by a factor of 0.75, relative to the Pauling[10] free ion electronic polarizability values.

In effect, these polarizability value variations differentiating between the ionic environmental patterns (crystal, ionic liquid, free ion) necessarily include changes in the neighboring force field overlaps[16], Madelung potentials[17] and the energy band effects[18].

Such direct environmental-behavioral patterns are shown in Table 2. For example, the smaller ionic radius (r_c/r_a) or the effective electron polarizability (α_c/α_a) ratios correspond to larger melting volume (V_m^s/V_m^l) ratios. Scrutiny of data found in Table 3 reveals that the geometric crystal lattice and the ionic liquid property ratios

TABLE 2

SUMMARY OF DATA

Alkali halide	ω_e (cm^{-1}) (*ref. 9*)	ΔH_f ($cal\ mol^{-1}$) (*ref. 21*)	T_t (K) (*ref. 21*)	U_0 ($cal\ mol^{-1}$) (*ref. 15*)	θ (K) (*ref. 22*)	ΔT (K)	α_c *and* α_a	$\frac{r_c}{r_a}$ (*ref. 10*)	$\frac{V_m^a}{V_m^i}$ (*ref. 23*)
LiF	910.25	6470	1121	246400	733.07	387.93	0.041 0.582	0.44	0.7594
LiCl	643.31	4720	880	202200	428.85	451.15	0.048 2.205	0.33	0.8000
LiBr	563.2	4220	823	190300	274.07	548.93	0.039 3.097	0.31	0.8188
LiI	498.2	3500	742	176200	—	—	0.038 4.797	0.28	0.8320
NaF	536.10	8030	1268	219600	491.85	776.15	0.256 0.614	0.70	0.7798
NaCl	364.6	6690	1073	188200	320.85	752.15	0.239 2.507	0.52	0.8132
NaBr	298.49	6240	1020	177200	224.36	795.64	0.227 3.585	0.49	0.8250
NaI	259.20	3640	933	165200	167.51	765.49	0.220 5.616	0.44	0.838o
KF	426.04	6750	1131	194300	332.84	798.16	1.052 0.784	0.98	0.8346
KCl	279.8	6270	1044	170300	236.10	807.90	1.053 2.750	0.73	0.8562

(Table continued on page 330)

TABLE 2 (*continued*)

Alkali halide	ω_e (cm^{-1}) (*ref. 9*)	ΔH_f ($cal\ mol^{-1}$) (*ref. 21*)	T_f (*K*) (*ref. 21*)	U_O ($cal\ mol^{-1}$) (*ref. 15*)	θ (*K*) (*ref. 22*)	ΔT (*K*)	α_c *and* α_a	$\frac{r_c}{r_a}$ (*ref. 10*)	$\frac{V_m^0}{V_m^1}$ (*ref. 23*)
KBr	219.17	6100	1007	163700	172.15	834.85	1.002 3.876	0.68	0.8620
KI	186.53	5740	954	153200	130.77	823.83	0.980 5.960	0.62	0.8694
RbF	373.27	5820	1068	189600	211.70	856.3	1.788 0.777	1.09	—
RbCl	233.34	5670	995	165600	168.80	825.2	1.681 3.009	0.82	0.8815
RbBr	169.46	5570	965	158300	136.34	828.66	— —	0.76	0.8866
RbI	138.511	5270	920	149900	107.81	812.19	— —	0.69	0.8903
CsF	352.56	5190	976	181000	—	—	3.181 0.731	1.24	0.9013[a]
CsCl	214.22	5840	918	160000	159.39	758.61	2.045 4.286	0.93	0.9106
CsBr	149.503	5640	909	153400	149.417	759.53	— —	0.87	0.9196[a]
CsI	119.195	5640	899	145300	126.21	772.79	2.880 5.866	0.78	0.9241[a]

[a]Estimated value (this work) from data given in ref. 23.

TABLE 3

CALCULATED CONSTANTS "a", "b" AND THE CORRESPONDING GROUP CORRELATION COEFFICIENT "r" (eq. (3))

Alkali halide class[a], *MX*	*Group I*			*II*			*III*			*IV*		
	a	*m*	r^b	*a*	*m*	r^b	*a*	*m*	r^b	*a*	*m*	r^b
LiX	−8.2740	−24.3184	−0.9998	−3.9690	−21.5785	−0.9997	−9.1753	−31.4310	−1.0000	−4.8277	−28.5287	−1.0000
NaX	−8.2361	−34.2148	−0.9993	−4.7223	−33.0924	−0.9992	−8.7441	−38.2589	−0.9999	−5.2305	−37.1379	−0.9999
KX	−7.6380	−49.9804	−0.9997	−4.4853	−50.5914	−0.9994	−8.1168	−45.5811	−0.9991	−4.9642	−55.1922	−0.9987
RbX	—	—	—	—	—	—	—	—	—	—	—	—
CsX	−18.0349	−197.2039	−1.0000	−17.2060	−222.9229	−1.0000	—	—	—	—	—	—

Alkali halide class[a], *MX*	*Group V*			*VI*			*VII*			*VIII*		
	a	*m*	r^b	*a*	*m*	r^b	*a*	*m*	r^b	*a*	*m*	r^b
LiX	2.5214	4.9702	0.9884	5.6077	4.4076	0.9870	4.1565	5.7028	1.0000	7.2731	5.1762	1.0000
NaX	2.1722	5.2635	0.9983	6.5845	6.8975	1.0000	2.8861	5.8711	0.9965	6.0592	5.6995	0.9966
KX	1.8518	5.4202	0.9999	4.7545	4.4522	0.9986	1.8514	4.8025	0.9981	5.1154	4.8554	0.9975
RbX	—	—	—	—	—	—	—	—	—	—	—	—
CsX	0.9362	7.0601	1.0000	4.2390	7.9809	1.0000	—	—	—	—	—	—

(*Table continued on page 332*)

TABLE 3 (*continued*)

Alkali halide class[a], *MX*	*Group IX*			*X*			*XI*			*XII*		
	a	*m*	r^b	*a*	*m*	r^b	*a*	*m*	r^b	*a*	*m*	r^b
LiX	1.9591	−2.3761	−0.9994	10.5315	−12.2660	−1.0000	−3.5976	13.0018	0.9992	0.1808	11.5343	0.9988
NaX	5.5881	−7.7923	−0.9871	12.0358	−15.3187	−0.9885	2.8411	5.3337	0.9798	5.9904	5.1570	0.9794
KX	15.1389	−18.8590	−0.9833	19.9521	−24.2035	−0.9816	2.9816	2.7340	0.9665	6.4896	3.0857	0.9891
RbX	48.9171	−56.7255	−1.0000	54.9105	−63.3137	−1.0000	—	—	—	—	—	—
CsX	38.1044	−43.0167	−0.9985	35.5941	−40.0778	−1.0000	5.4965	4.6481	1.0000	9.3940	5.2542	1.0000

Alkali halide class[a], *MX*	*Group XIII*			*XIV*		
	a	*m*	r^b	*a*	*m*	r^b
LiX	0.7108	14.8623	1.0000	−0.6150	2.9903	1.0000
NaX	6.8097	5.8131	0.9845	3.7067	2.9662	0.9851
KX	7.0184	3.33769	0.9914	5.6371	2.6236	0.9903
RbX	—	—	—	—	—	—
CsX	—	—	—	—	—	—

[a]Alkali halide class is designated by MX where M = Li, Na, K, Rb, Cs; while X = F, Cl, Br, I.
[b]The correlation coefficient "r" is defined as:

$$r = \frac{\sum_{i=1}^{n} (X_i - \overline{X})(Y_i - \overline{Y})}{\sqrt{\sum_{i=1}^{n} (X_i - \overline{X})(Y_i - \overline{Y})^2}}$$

where: $\overline{X} = \frac{\sum_{i=1}^{n} X_i}{n}$ and $\overline{Y} = \frac{\sum_{i=1}^{n} \overline{Y}_i}{n}$ while n is the number of data points.

(r_c/r_a; V_m^s/V_m^l) are proportional to the dimensionless energetic state properties (ΔH_f, U_0) when those are modified by the effective electronic polarizability ratio α_c/α_a. These proportionalities then establish our proposed A–τ correlation (eqn (1), Figs. 1–4 Table 3) sets and are in effect the energetic–geometrical description of the melting process referred to as either the melting point, T_f, or to the Debye temperature, θ; in such a way as to involve the temperature range ΔT, defined as $\Delta T = T_f - \theta$; i.e., the temperature difference between the melting point T_f and the Debye temperature θ of the alkali halide. The melting temperature T_f is usually larger than the corresponding Debye temperature θ. This permits to separate the anharmonic thermodynamic property behavior region from the region characterized by the quantum mechanical Debye temperature θ-states. This differentiation appears to be significant in the case of the crystal lattice cohesive energy U_0 correlations Figs. 1–4 (Table 3):

$$\ln\left(\frac{U_0(\alpha_c/\alpha_a)}{R\Delta T}\right) \text{ vs. } \ln\left(\frac{hc\omega_c}{k\Delta T}\right); \qquad \ln\left(\frac{U_0(\alpha_c/\alpha_a)}{R\Delta T}\right) \text{ vs. } \ln\left(\frac{r_c}{r_a}\right)$$

$$\ln\left(\frac{U_0(\alpha_c/\alpha_a)}{R\Delta T}\right) \text{ vs. } \ln\left(\frac{V_m^s}{V_m^l}\right);$$

especially for the $\ln\left(\frac{U_0(\alpha_c/\alpha_a)}{R\Delta T}\right)$ vs. $\ln\left(\frac{hc\omega_c}{k\Delta T}\right)$ relation. It should be noted that Debye temperature θ alone does not correlate; only when referred to the temperature difference $\Delta T = T_f - \theta$. Table 3 and Figs. 1–4 reveal that the heat of melting, ΔH_f, relations when compared to the crystal lattice energy, U_0, relations are nearly parallel to (nearly the same slope) although always lower (smaller constant "a" value) than the corresponding crystal lattice energy, U_0, relations. For the same alkali halide class, MX, and fixed thermodynamic state, this particular ΔH_f vs. U_0 relation shift along the A-coordinate demonstrates the validity and restrictions as set forth by the energy conservation principle expressed through the use of the Born–Fajans–Haber thermochemical cycle.

It remains an open question whether at the melting point there could be established energetic–geometrical property correlation common for all MX-class alkali halides. Figure 5 representing

$$\ln\left(\frac{\Delta H_f(\alpha_c/\alpha_a)}{RT_f}\right) \quad \text{and} \quad \ln\left(\frac{U_0(\alpha_c/\alpha_a)}{RT_f}\right)$$

plots versus (r_c/r_a) ratio (note that the ionic radii, r_c and r_a, are given by means of 3 sets: Pauling[10] and the minimum density and overlap[19] values) seems to be the closest approach yielding a unique correlation* between the energetic and lattice geometry characterizing parameters during the melting process of alkali halides.

*Furukawa[20] in his attempt to obtain a common property equation for all halides at the melting point has not entirely succeeded. For instance, Furukawa's[20] relation, $\Delta Hc_{o_p}RT_m = f(r_c/r_a)\ (\alpha)^{1/3}$, where $\alpha = \alpha_c + \alpha_a$ and T_m is melting point temperature, seems to imply that the dimensionless energy ratio $\Delta H_{o_p}/RT_m$ becomes equal to the length unit in Ångstrøms.

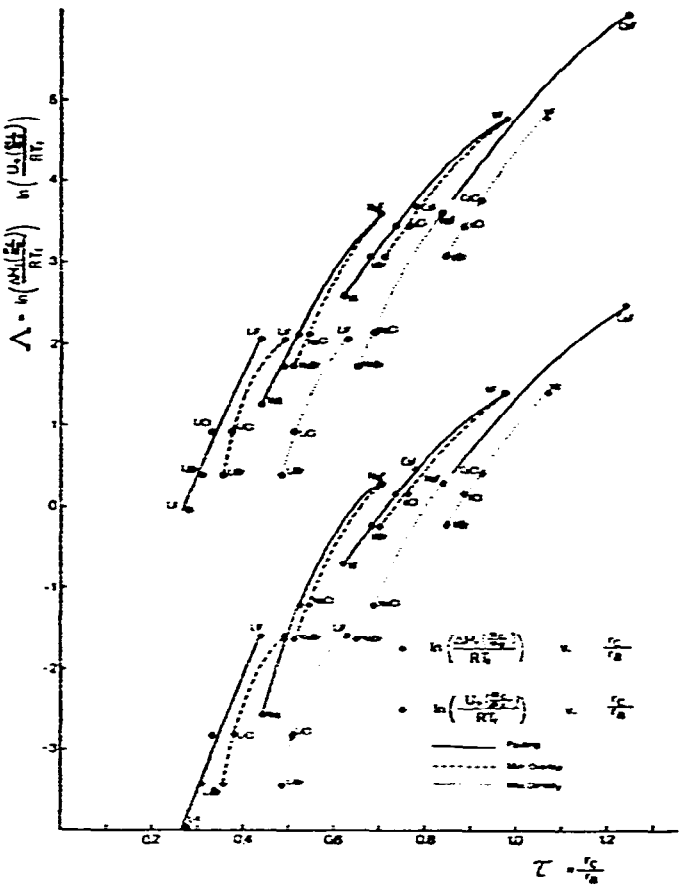

Fig. 5. Comparative $\Lambda = \ln\left(\frac{\Delta H_f(r_c/r_a)}{RT_f}\right)$ vs. $\tau = \frac{r_c}{r_a}$ and $\Lambda = \ln\left(\frac{U_0(r_c/r_a)}{RT_f}\right)$ vs. $\tau = \frac{r_c}{r_a}$ plots representing three sets of obtained ionic radius ratio (r_c/r_a) data: Pauling, minimum overlap and maximum overlap[19]. As seen, the general behavior of the resulting curves is similar; except for slight upwards shift. Note that Tables 1–3 display the obtained linear $\Lambda = a + m\tau$ relations.

We may rewrite eqn (3) as functional expression:

$$\Lambda(\varepsilon) = m\tau(g) + a \tag{6}$$

where ε represents characteristic energy, while g is a geometry describing parameter or parameter ratio; m and a retaining the previously assigned meaning.

If we now consider X-ray and neutron scattering interference patterns for unlike (metal–halogen) and like (metal–metal; halogen–halogen) ions; and if we designate the nearest ionic distances for unlike ions r_1^l and r_1^s; for the liquid and solid states; and the associated coordination numbers as n_1^l and n_1^s, respectively; while for like ions we write for the same cases r_2^l, r_2^s, n_2^l, n_2^s, correspondingly; then, we may write[20] the geometric relation:

$$\frac{V_m^s}{V_m^l} = \left(\frac{r_1^s}{r_1^l}\right)^3 \frac{n_1^l}{n_1^s} \tag{7}$$

Comparing eqns (7) and (6), we find that V_m^s/V_m^l relates to $\tau(g)$ and hence to the characteristic energy term, $A(\varepsilon)$. Experimentally, we know the proportionality between r_1 and r_2; and n_1 and n_2 (ref. 20); and so we have relationships between the characteristic energies of melting and the alkali halide lattice; and the interference patterns, and the coordination numbers of ions in the liquid and solid state.

Clearly, the presented relations (eqn (3); Figs. 1–4, Table 3) connecting the energetics and the lattice geometry (eqns (6) and (7)) may present an intuitive understanding of the melting process and resulting structure of the ionic liquid.

ACKNOWLEDGEMENT

The financial assistance of the National Research Council is gratefully acknowledged.

REFERENCES

1 F. A. Lindemann, *Phys. Z.*, 11 (1910) 609.
2 E. Grueneisen, *Ann. Phys.*, 39 (1912) 257.
3 W. Braubeck, *Z. Phys.*, 38 (1926) 549.
4 N. V. Raschevsky, *Z. Phys.*, 40 (1927) 214.
5 J. Frenkel, *Kinetic Theory of Liquids*, Oxford, New York, 1946.
6 J. E. Lennard-Jones and A. F. Devonshire, *Proc. Roy. Soc.* A, 169 (1939) 317.
7 L. Brillouin, *Phys. Rev.*, 54 (1938) 916.
8 M. Born, *J. Chem. Phys.*, 7 (1939) 591.
9 P. Brumer and M. Karplus, *J. Chem. Phys.*, 58 (1973) 3903.
10 L. Pauling, *The Nature of the Chemical Bond*, Cornell University Press, 1960
11 J. Lielmezs, *J. Inorg. Nucl. Chem.*, 36 (1974) 3773.
12 J. Lielmezs and H. J. Vogt, *Thermochim. Acta*, 6 (1973) 27.
13 J. Lielmezs, *J. Quant. Spectr. Radiat. Transf.*, 11 (1971) 1749.
14 K. Fajans, *Z. Kristallogr.*, 61 (1925) 18.
15 M. F. C. Ladd, *J. Chem. Phys.*, 60 (1974) 1954.
16 A. R. Ruffa, *Phys. Rev.*, 130 (1963) 1412.
17 E. Paschalis and A. Weiss, *Theor. Chem. Acta*, 13 (1969) 381.
18 M. I. Petrashon, I. V. Abarenkoff and N. N. Kristofel, *Opt. Spectra*, 9 (1960) 276.
19 V. M. Maslen, *Proc. Phys. Soc.*, 91 (1967) 259.
20 K. Furukawa, *Disc. Faraday Soc.*, 32 (1961) 53.
21 L. Brewer and E. Brackett, *Chem. Rev.*, 61 (1961) 425.
22 A. Konti and Y. P. Varshni, *Can. J. Phys.*, 49 (1971) 3115.
23 H. Spindler and F. Sauerwald, *Z. Anorg. Allg. Chem.*, 335 (1965) 267.